

Correlation between Quantitative and Qualitative Analysis on Image Quality of Digital Dental X-ray Images

Siti Arpah Ahmad^{1,2}, Mohd Nasir Taib², Noor Elaiza Abdul Khalid¹ and Haslina Taib³

¹Faculty of Computer and Mathematical Science, Universiti Teknologi MARA, Malaysia,

²Faculty of Electrical Engineering, Universiti Teknologi MARA, Malaysia,
40450 Shah Alam, Selangor Malaysia

³School of Dental Sciences, Health Campus, Universiti Sains Malaysia, Kubang Kerian,
Kelantan, Malaysia,

arpah@tmsk.uitm.edu.my, elaiza@tmsk.uitm.edu.my, drnasir@ieee.org, haslina@kck.usm.my

Abstract: Signal to Noise Ratio (SNR) is a quantitative method to measure the effectiveness of contrast enhancement methods. The question is whether this measurement is consistent with a qualitative evaluation of a medical expert. Biomedical Research, including dentistry cases, usually involves medical experts to do the interpretation, and finalize the diagnosis. However, the subjective evaluations create differences of interpretation. There are two factors contributing to the low quality of dental radiographs—the first is because of the nature of the image acquisition process, and the second is the low X-ray dose usage. Due to that, research related to contrast enhancement algorithms is an accepted image processing method to assist medical officers in doing interpretation that is more reliable. Thus, this work presents an analysis of contrast enhancement algorithms (CEA) applied to digital intraoral radiograph images. The enhancement methods used in this study are CEAs, namely: adaptive histogram equalization (AHE), contrast limited adaptive histogram equalization (CLAHE), and sharp contrast limited adaptive histogram equalization (SCLAHE). The objective of this work is to find a correlation between the dentist evaluation and SNR values in determining the image quality based on the rate of abnormalities detected. Fifty-six original intraoral digital dental X-ray images are collected from the Faculty of Dentistry, Universiti Teknologi MARA Malaysia. These images are processed with the mentioned CEAs, resulting in a total of one-hundred sixty-six observations. These images are compared against the original images. The method of assessment is through questionnaires where all images are arranged randomly. The observations focused on identifying widened periodontal ligament space (widened PDLs), periapical radiolucency (PR) and loss of lamina dura (loss LD) abnormalities. These are among the main signs of periapical disease. The results show that the SNR value does not reflect the dentist's evaluation in terms of image quality. The SNR values of CLAHE are able to precede other methods. However, SCLAHE is better than the rest based on dentists' evaluations for widened PDLs abnormality.

Keywords: image enhancement, signal to noise ratio (SNR), dental X-ray, compound enhancement algorithm (CEA)

1. Introduction

Signal to Noise Ratio (SNR) is an accepted quantitative analysis in evaluating the performance of enhancement techniques [1-3]. The enhancement techniques are an accepted image processing task in medical imaging [1-16]. Medical images need image processing techniques to

enhance the visual appearance of the images [1][3][4-12]. The images suffer low contrast due to low X-ray dose usage [13][17-18]. Aside from that, the nature of image acquisition also contributed to noise that degrades the image quality [13]. The SNR provides measurement for image quality in terms of image details [2]. The higher the SNR values, the better the performance of the enhanced images [1].

Qualitative analysis was used with questionnaires/survey that measured an observer's evaluation in quantifying the image quality [6-12]. Attention also was given to the issues of inter- and intra-observation of expert evaluation on the resultant image between the enhanced methods and original images. However, it is expensive to have experts answer the questionnaire and it is also time consuming. Due to that, the number of them usually is small. Usually, the surveys included one radiologist [19], three to five dentists [2-3][10][14] and postgraduates with experience in oral and maxillofacial radiology including digital radiography [4]. The number of image samples used ranges from 12 to 42 panoramic radiographs [1], periapical digital radiographs [2][4], interproximal radiographs [3] and bitewing [4] images. The survey usually involves a five-point scale. However, preliminary results by Sund and Moystad suggested that the five-point scale was not warranted [10]. Due to that, a three-point scale is common and has been utilized in many surveys related to medical imaging [19-23]. Usually the radiologists were asked to assess the quality of the images before and after certain techniques had been applied [8-12]. For example, a three-point scale has been used in research related to the improvement of image quality of computed tomography (CT) after the utilization of an accreditation program [21], the CT dose reduction techniques aimed at preserving image quality in reducing radiation dose [22], and the evaluation of the usefulness of contrast-enhanced three-dimensional magnetic resonance (MR) angiography [23].

Results from surveys related to dentistry research typically are evaluated using statistical techniques such as Kruskal-Wallis, odd ratio, Cohen's Kappa [2], mean, standard deviation (SD) [1][11], linear regression, one-way ANOVA[7] and the Wilcoxon sign rank test [8][24-26].

The Wilcoxon signed rank test is designed to be used with repeated measurements; for example, the same sample under

two different conditions [27]. For example, this technique had been used to see the difference in diagnostic grade for both upper and lower jaw before and after histogram equalization operation [8]. Other examples that used the Wilcoxon test are as follows: comparison between before and after a certain chemical had been applied to the dental ceramic [24], clinical comparison of the efficacy and efficiency of professional prophylaxis procedures in orthodontic patients [25] and research related to pharmacokinetics of bisphenol from a dental sealant when applied in different dosages [26].

One of the common diseases in dentistry is periapical disease that occurs at the apices of the teeth. The diagnosis of this disease is particularly valuable to enable the clinician to provide immediate and appropriate dental treatment [14]. Frequently encountered periapical diseases are granulomas and cysts that appear at the jaw. Other lesions, including nondontogenic and malignancies, are also noteworthy lesions that relate to periapical disease [15]. Pathology/signs that may be presented in this disease are periapical radiolucency, widening periodontal ligament space, and the loss of lamina dura surrounding the teeth [14].

Currently, intraoral radiography film is the only common way to diagnose periapical pathology in routine clinical practice [14][16]. These lesions can be detected in the radiographic images based on the degree or gradation of “blackness” of the radiograph images [15]. The term radiolucent (dark/black) and radiopaque (light/white) are used in ordinary-ray images such as intraoral, panoramic, and extraoral radiograph. The interpretation of the radiographs is based on the appearance of the tissues. The tissues that tickler, more mineralized or denser, is known as radiopaque [28]. Figure 1 shows the structures surrounding the root of the teeth in the periapical X-ray images. The radiopacity shows the soft tissues such as periodontal ligament space (1), pulp chamber (2), root dentine (3), periapical area (4) and lamina dura (5).

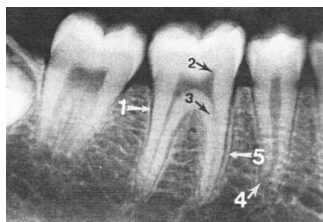


Figure 1. Intraoral periapical radiograph of teeth at lower right jaw [28].

Another example of lamina dura can be seen below in Figure 2.



Figure 2. Lamina dura [28].

Figure 3 shows the periapical radiolucency present at tooth upper lateral incisor as indicated by the arrows [15].

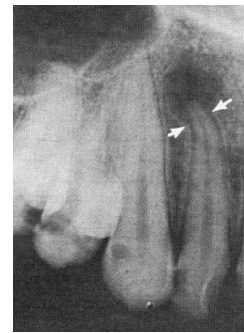


Figure 3. Intraoral periapical radiograph of upper teeth [28].

Figure 4 exhibits the periapical radiolucency abnormality. Take note of the black or dark gray areas around the apices of the teeth [28] that the arrow points to in Figure 4 (a) and (b) [18].

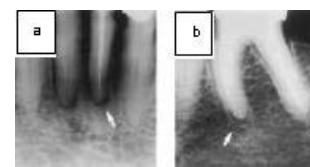


Figure 4. Example of periapical radiolucency [29].

Issues related to dental radiograph interpretation are based on the nature of the technique of the X-ray machine. An intraoral radiograph image is produced by X-rays passing through an object and interacting with photographic emulsion on film. X-ray images are produced by the strength of rays that pass through the anatomical structures of the human body. Higher anatomical density will reduce the strength of the rays, making it appear white indicating the bone areas, whereas, the soft tissue areas appear dark. Thus, the final radiographic image can be described as a two dimensional image resulting from a combination of black, white, and grey superimposed shadows. However, the teeth are three dimensional objects and the shadows cast by different parts of an object are superimposed upon each other on the final radiograph. In this situation, the invisibility of a particular feature does not mean that the feature does not exist, merely that it cannot be seen [4]. The superimposition problem affects the periodontal ligament space [11], lamina dura [8], and condition of alveolar bone [9] pathologies.

This limitation on conventional radiographic images has significant clinical implications, which could lead to misdiagnosis [15]. Cases of misdiagnosis in dentistry do happen [29-31]. The varying morphology of apical areas and varying density of surrounding bone present uncertainty in radiograph decision making [29]. This situation needs more attention and careful analysis of periodontal ligament space and the lamina dura pathologies [29]. The clinicopathological features contribute to radiographic similarity and could lead to misdiagnosis, especially between periapical giant cell lesions and endodontic lesions [30]. The fuzziness of X-ray film also produces doubt for diagnosis of boundary line at the apical lesion [31]. Aside from the mentioned drawback, another factor that affects the evaluation of periapical disease is the variation in dentists' assessments [29][32-33]. For example, research by Lanning [34] had reported that there is significant variability in periodontal diagnosis and treatment planning among dental

schools [34]. There also is disagreement in the borderline cases in the method of doing the radiographic diagnosis of the disease [29]. However, past research showed that software enhancement tools that adjust contrast, density, image size, etc., do contribute to the closeness in diagnoses among observers [32].

As mentioned earlier, contrast and density, do influence the radiographic image quality. This work focuses on contrast. Contrast is the visual difference between the various black, white, and grey shadows that exist in the image. The contrast between adjacent structures can alter the perceived density of one or both of them [4]. Low contrast effect did occur in periapical disease detection. For example, widening periodontal ligament space at the upper molar usually has low contrast and structure generally not easily seen by the naked eye [11]. This is due to the overlying bone, which reduced the dose in the detector plane to a level where the slope. Therefore, the contrast characteristic S-shape curve is low [11].

In overcoming the mentioned problem about low contrast in the images, the contrast enhancement technique is a well known and accepted method in assisting medical experts in doing the disease diagnosis [4-6]. This technique manipulates the black and white in the images, which may alter the perceived visual appearance of the images [4]. The global approach, termed a histogram equalization (HE), enhanced the original image through brightness intensity distribution applied to the whole image [6][35], which makes the image become over-enhanced and look unnatural [36]. Due to this effect, the use of the adaptive histogram equalization (AHE) is introduced [6][35-36]. This approach overcomes the drawback of HE but produces a washout effect [37] and introduces artifacts [36]. Thus, the creation of the contrast limit histogram equalization (CLAHE) limits local contrast-gain by restricting the height of a local histogram [38]. However, the CLAHE problem is related to high contrast in both foreground and background. This effect increases the visibility of the main mass that creates some intensity yet could be mislead in the background's homogeneities [39].

All of these drawbacks encourage the combination of HE, AHE and CLAHE with other algorithms [1][35][37][40-43]. The sharpening filter often is combined with classic contrast enhancement methods [41-43] to enhance medical images [37][41][43]. Aside from the sharpening filter, the median filter also is applied to medical images [44-48] but none to dental X-ray images.

As in the dentistry field, contrast enhancement methods are termed filters and applications to dental radiographs are many [7-11]. The contrast enhancement methods are created using software that comes with the X-ray machines such as Digora for Windows [7], Photoshop 8.0 [8], and Trophy Windows [9], a self-developed algorithm called the sliding window adaptive histogram equalization (SWAHE) [10] and frequency domain algorithms [11]. Two main image processing functions that have been used are high-pass filters and contrast enhancement. The high pass filter types that have been used are shadow [7] and sharpening [7][12]. Research regarding medical data as input data and using contrast techniques to enhance the original images is common [3][5-12][38][49]. The medical images used usually

are mammograms for breast cancer [5] [38-39][49] as well as dental radiographs [3][6-11]. Focusing on dentistry, the abnormalities being investigated were periodontal ligament space [11], lamina dura [8] and condition of alveolar bone [9]. Many types of contrast enhancement variations have been used. For example, adaptive histogram equalization (AHE) [8], bright contrast enhancement [8], and pseudo-colored with brightness-contrast adjustment [8]. Negative or inversion algorithms had been used in [7][9] to test the effects of brightness changes in the dark region of the image.

The effectiveness of certain contrast enhancement methods needs to be measured. SNR has been used in application on ultrasound [50], computed tomography (CT) [51] and dental X-rays [3][6]. Aside from SNR as the performance indicator, many other quantitative measurements had been applied to quantify the success of certain contrast enhancement techniques [49][52-53]. Methods such as calculating the edge pixel have been used to compare mammogram images to the enhanced images by six edge detectors [52]. The fuzzy rule-based algorithm had been used to perform contrast enhancement on mammograms on breast cancer masses [49]. They applied the concept of mean grey scales ratios between the target and background images of the original and enhanced images. In dentistry-related data, Hazem and Mastorakis, [54] used two dental images to test a new algorithm termed a fast neural network (FNN), in detecting dental disease, which focuses on mathematical proof. Our previous work [3][6] uses contrast improvement index (CII), root mean square error (RMSE) and SNR to quantify SCLAHE, which is shown as performing slightly better than the original images.

Based on the above introduction, the importance of SNR is obvious. However, does this value tally with the dentists' or medical experts' visual evaluation? This question arises based on the review of research done specifically in the area of dentistry [7-12]. Attention is given to issues of inter- and intra-observation of expert evaluation between the resultant enhanced and original images.

Based on the review above, our work intends to investigate how quantitative measurement, namely SNR, can correlate with dentists' qualitative evaluations in analyzing the performance of images enhanced by CEAs in detecting periapical disease abnormalities.

2. Material and Method

2.1 Material

Fifty-six intraoral digital radiograph images were taken from Faculty of Dentistry Universiti Teknologi MARA, Malaysia. The X-ray machine used was the Planmeca (German) Intraoral machine. This machine used imaging technology, namely cone beam volumetric tomography (CBVT), with an image matrix of 1516 X 1900 pixels and pixel size is 127 μ . Originally, these images were in the form of film. Then the images were converted to digital form in .tif format using a Scanmaker 1000x Microtec machine. Later, for easy manipulation, they were converted to Bitmap format (bmp).

2.2 Research Methodology

The flow chart of this work is shown in Figure 5. The work starts with the literature review as presented in the previous

section. Then the original intraoral dental radiograph images were collected. Next, the application of CEAs is done, followed by the dentist's evaluation. Finally, the analysis is pursued.

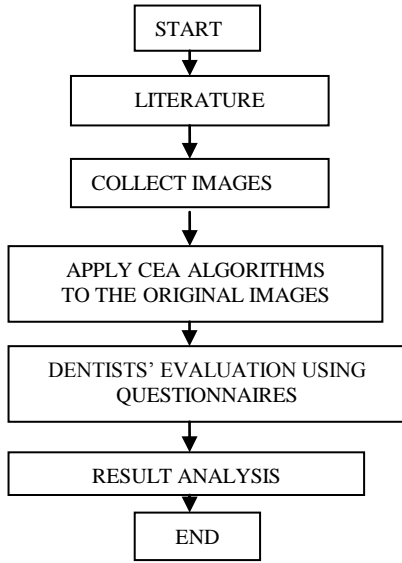


Figure 5. Research methodology flowchart

2.3 Application of CEAs

The basic contrast enhancement algorithms used are histogram equalizations (HE) [55]. The concept of this algorithm is to enhance the image by remapping the image intensity values by using equation [56].

$$G_i = \left\lfloor \sum_{j=0}^i N_j \right\rfloor \left(\frac{\max \text{Intensity Level}}{\text{NoofPixels}} \right) \quad (1)$$

Because of the drawback of HE, it evolved into AHE. Figure 6 shows the AHE processing stages for this work. Noted in the figure, the original image's histogram is skewed to the left. The operation of AHE started with partitioning the image into a 3X3 mask. Then the AHE operation is done. After the operation, it is clearly seen the flatter a histogram of the images of the partition as well as after the interpolation.

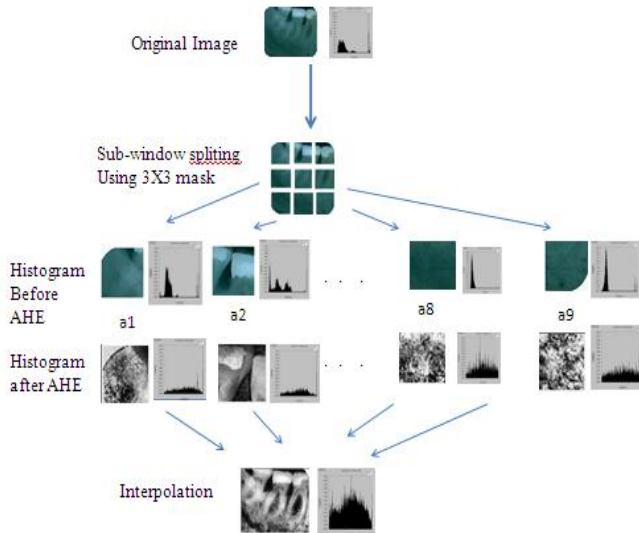


Figure 6. Basic stages of AHE processing

Due to the disadvantage of AHE, the CLAHE was introduced. Figure 7 shows the differences between the three standards (HE, AHE and CLAHE). Figure 7 (a), illustrates the histogram transformation from original image to HE. Figure 7 (b), shows AHE operation where, the operation of HE is done locally in the predefined window size. Figure 7 (c) illustrates how random noise in the local histogram equalization is discarded by limiting the maximum slope of the grayscale transform function used in the CLAHE algorithm. The algorithm clips the histograms or bin that exceeded the threshold. It then redistributes the excess evenly among all of the remaining bins [57]. The AHE, CLAHE, and SCLAHE algorithms are termed contrast enhancement algorithms (CEAs) because all of the methods originated from the same concept.



Figure 7. The differences between HE, AHE and CLAHE [58]

The SCLAHE algorithm is the combination of spatial filtering, which is the sharpening algorithm, and the histogram equalization. The sharpening algorithm originates from the spatial domain and can be expressed by the equation [59] below:

$$g(m, n) = T(f(m, n)) \quad (2)$$

where $(f(m, n))$ is the input image, $g(m, n)$ is the enhanced image. T is the operator that defined the modification. The proposed algorithm utilized a Laplacian filter as T . Laplacian detects the outlines of objects by convolving a mask with a matrix centered on a target pixel. The Laplacian detects the edge using a mask as in Figure 8 [60]. Then, it modifies the histogram to enhance the contrast of the pixels within the sub-images [60].

	-1	
-1	4	-1
	-1	

Figure 8. Laplacian edge detection

2.4 Dentist's Evaluation

The questionnaire had been used to evaluate the performance between the original and the enhanced image by CEAs. The method for viewing the questionnaire was one image per evaluation and the arrangements between all images were random. Previous work used the "twin view" [3][6][14] approach. A dentist was assigned to evaluate the quality of images by focusing on the ability of the images to detect the presence of periapical radiolucency (PA) abnormality, widened periodontal ligament space (widened PDLs) abnormality, and loss of lamina dura (loss of LD) abnormality. To check the reliability of the dentist's

assessments, a preliminary study had been conducted using 10 images. The dentist evaluated the same images two times. This was known as first reading and second reading [9]. The evaluation was on the original and SCLAHE only. The statistical test used was the Wilcoxon sign rank test. The exact assessment scores were as follows; class=1: Widened periodontal ligament space (widened PDLs) detected, class=2: No widened periodontal ligament space detected but other abnormality detected and class=3: No widened periodontal ligament space detected and no abnormality detected. The questions were the same for the other two abnormalities, which are periapical radiolucency (PR) and loss of lamina dura (loss LD).

2.5 Quantitative Measurement - SNR

The Signal to Noise ratio (SNR) had been chosen to evaluate the performance between the CEAs. The values were obtained by comparing the CEAs to the original images. Below is the equation of SNR [3];

$$SNR = 10 \log_{10} \left[\frac{\sum_{x=0}^{n_x-1} \sum_{y=0}^{n_y-1} [r(x,y)]^2}{\sum_{x=0}^{n_x-1} \sum_{y=0}^{n_y-1} [r(x,y) - t(x,y)]^2} \right] \quad (3)$$

where, $r(x,y)$ represent the original image, and $t(x,y)$ is the enhanced image by CEAs. The values are represented in decibel (dB) units.

3. Results

Results are presented in the following manner; section 3.1 (a) is the result of the preliminary study on the accuracy of the dental assessment. Section 3.1 (b) is the comparison between original and CEAs by class, in detecting the abnormalities. Section 3.1 (c) shows the results that compare the occurrences of abnormalities per image in the 216 observation by the dentist. Section 3.2 shows the correlation of SNR toward the dental evaluation on the performance of the CEAs based on classes. Section 3.3 is about the trend of median of SNR values for class=1 for each of the abnormalities. Finally, section 3.4 shows the overall results.

3.1 Comparison based on dental evaluation on abnormalities

a) First and second reading

Results of the first and second reading were checked using the Wilcoxon for nonparametric analysis. The analysis was for two related samples (1st and 2nd reading) and SPSS was used for statistics. Results show that there is no significant different between the dentist's scores in the 1st and 2nd reading for PA abnormality ($z=0.000$, $p > 0.005(1)$, $median=1$), widened PDLs abnormality ($z=-2.349$, $p > 0.005(0.019)$, $median=1$) and loss of LD abnormality ($z=12.333$, $p > 0.005(0.02)$ $median=1$)

b) Comparison between original and CEAs by class, in detecting the abnormalities.

Figure 9 is about all of the abnormality in the images. For widened PDLs abnormality, the figure shows that, for class=1, SCLAHE has the highest scores with 36 images.

CLAHE is the second highest (33), followed by the original (31), and last is AHE (24). Class=2 shows the lowest score between the classes with CLAHE having the highest score (4), and SCLAHE having the lowest (1). Class=3 shows that AHE has the highest scores (29) and the original has the lowest (22). CLAHE (19) and SCLAHE (18) are only slightly different.

Next is the result of PR abnormality. For class=1, the figure shows that CLAHE and SCLAHE have the same score (18). The original images (25) is the highest and AHE is last (15). Class=2 shows that CLAHE has the highest score (22), followed by AHE (19), then SCLAHE (18), and the original images are the lowest (12). Class=3 shows that original and SCLAHE have the same score (19). AHE is the highest (21) and CLAHE has the lowest score (16).

The final result is about loss of LD abnormality. For class=1, CLAHE (24) is able to overcome SCLAHE (20). The ranking then goes to the original images (16), and AHE is the lowest (12). For class=2, the scores show that SCLAHE and AHE are the highest (3) then the original (2) and CLAHE (2). For class=3, the results show that AHE is the highest (40). The trend is then followed by the original (38), SCLAHE (32) and the lowest is CLAHE (30).

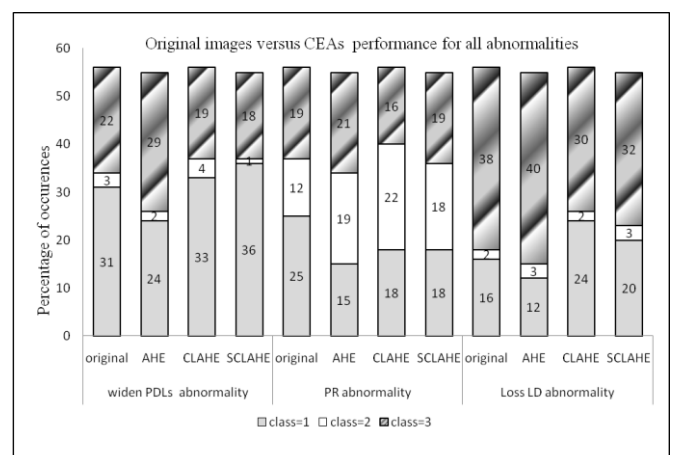


Figure 9. Original images versus image enhanced by CEAs performance by class in detecting all of the abnormalities

c) Comparison between classes by the occurrences of abnormalities per images.

Figure 10 shows that of 224 observations (original and CEAs), for class=1, the widened PDLs abnormality has the highest scores (124). The PR abnormality is second (76), and loss LD is the lowest (72). For class=2, PR has the highest scores (71). Widened PDLs and loss LD have the same scores (10). For class=3, loss LD is the highest (140); the second is widened PDLs (88) and the lowest is PR (75). Each of the abnormalities has two missing scores or no score was made by the dentist.

3.2 Average SNR values characteristics between classes for each of the abnormalities

This section focuses on SNR correlation toward the dentist's evaluation on the performance of the CEAs based on class. Figure 11 displays the average of the SNR values for all of the abnormalities. The first is about the widened PDLs abnormality. The result indicates that the highest average SNR values for each CEA come from class=3, where AHE is

9.63 dB, CLAHE is 24.72 dB and SCLAHE is 22.98 dB. Comparison between CEAs shows that CLAHE have the highest values for all classes. Next shows the average SNR values for PR abnormality.

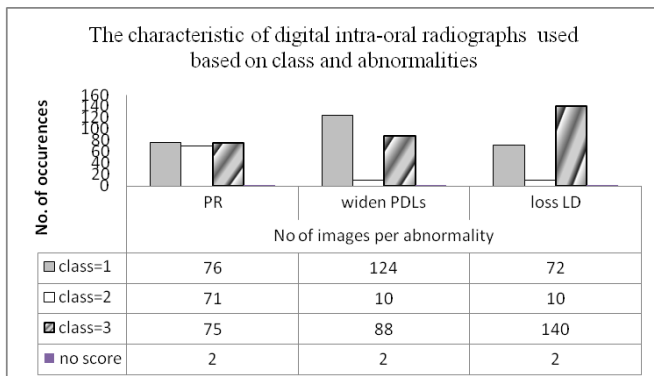


Figure 10. Digital intraoral characteristic based on class and abnormalities

The results show that class=3 has the highest SNR values, the average of which is 25.37 dB from the CLAHE. Overall performance for class=1 and class=2 of CEAs indicates that CLAHE has the highest SNR, followed by SCLAHE and last is AHE. Finally, the graph shows the results for loss LD abnormality. The trend is the same where class=3 has the highest SNR for CLAHE (25.46 dB). The trend is the same for class=1, but not for class=2.

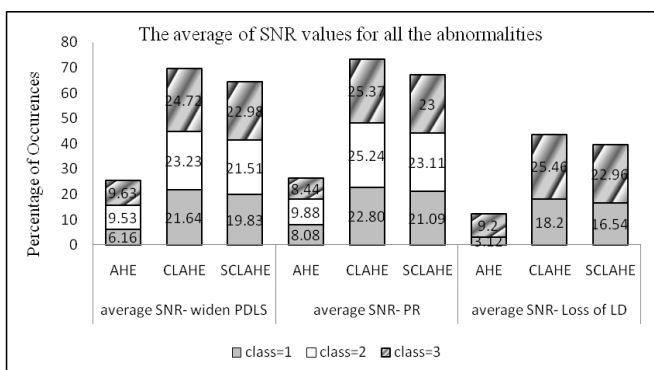


Figure 11. The average of SNR values for all of the abnormalities

3.3 The Correlation of average SNR values toward Dental Evaluation of the CEAs performance.

This section shows the trends of median of SNR values for class=1 only. The selected images are the images that have the same image reference for AHE, CLAHE, and SCLAHE.

Figure 12 shows that there are 14 images for widened PDLs abnormality, 8 images for PR abnormality and 7 images for loss LD abnormality. The median SNR values for AHE are approximately 8dB for all of the abnormalities. CLAHE and SCLAHE median SNR values are similar and approximately 21 to 23 dB. However, the CLAHE median SNR values (23dB) are better and more consistent than SCLAHE (21 to 22dB).

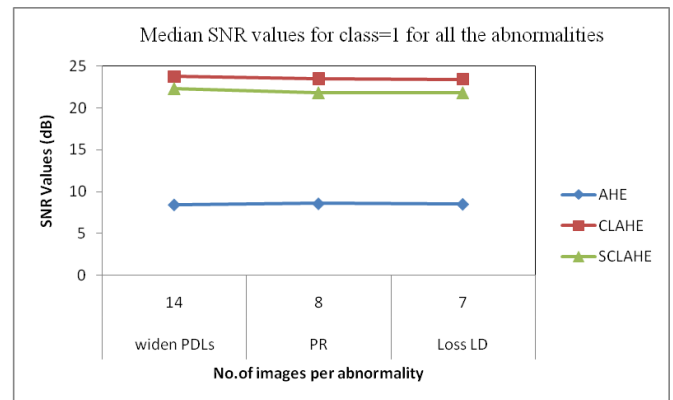


Figure 12. Median SNR values for class=1 for all of the abnormalities

3.4 Overall Results

This section consists of the summaries of average SNR values between CEAs.

Figure 13 displays the highest SNR values obtained. The first CEA is AHE. The highest values come from PR abnormality with class=1 is 8.08 and class=2 is 9.88 dB. Class=3 come from widened PDLs abnormalities with 9.63 dB.

Next is focused on CLAHE. It shows, for class=1, the highest value to come from loss LD abnormality (25.46 dB). For class=2 and class=3, the highest average SNR values come from PR abnormality with 25.24 dB and 23.11 dB.

The last CEA is SCLAHE. It indicates that the highest for all classes come from PR abnormality with class=1 is 21.09 dB. Class=2 is 23.11 dB and class=3 is 23 dB.

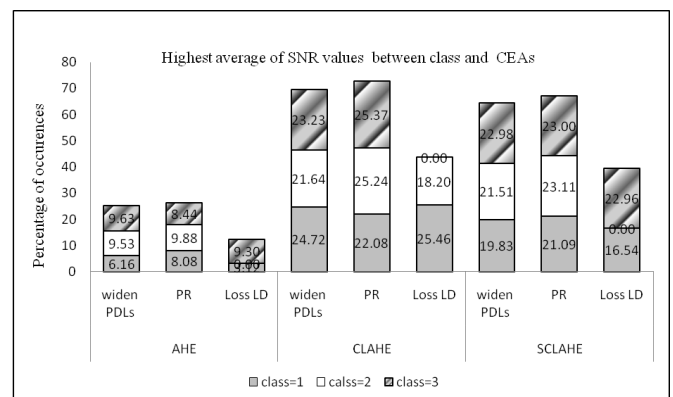


Figure 13. The highest average of SNR values between class and CEAs

Table 1 is the summary of average SNR values for class=1 for all of the abnormalities. The comparison is focused on the performance between CEAs. The table shows the SNR values and total score values are in the bracket. The table demonstrates that the trend is still the same with CLAHE the highest, followed by SCLAHE and AHE last. The highest average SNR is obtained by PR abnormality (22.80 dB).

4. Discussion

This work examines the correlation between the qualitative value of a dentist's evaluation and the quantitative values of SNR. The comparison is between digital intraoral dental images enhanced by CEAs and the original images.

Table 1. Comparison between SNR values and score for class=1 for all of the abnormalities

	AHE	CLAHE	SCLAHE
Widened PDLs	6.16 (24)	21.64 (33)	19.83 (36)
PR	8.08 (15)	22.80 (18)	21.09 (18)
Loss of LD	3.12 (12)	18.20 (24)	16.54 (20)

Psychophysical experiments signify that photographic and radiographic images with enhanced edges often are more pleasing to the human visual system than original images [7]. This statement is consistent with the finding for widened PDLs. It shows that SCLAHE is able to overcome originals and other enhanced images in detecting widened PDL abnormalities. Detecting this lesion is critical since this symptom is reported as a first step that could lead to cancer [61]. As for PR and loss of LD abnormalities, CLAHE shows superiority overall.

SNR values that have better visibility were said to be approximately 20db [62]. Based on that, even SCLAHE has SNR values lower than CLAHE (Table 1). Its values can still be considered acceptable since it was graded as class=1 (widened PDLs are detected) by the dentist.

Focusing on the dentist's evaluations with the SNR values obtained (Table 1), there is consistency between the two parameters for CLAHE and SCLAHE. However, the SNR values obtained by AHE are not consistent with the literature [62].

5. Conclusion

In conclusion, this investigation shows that in terms of SNR values, CLAHE precedes AHE and SCLAHE. However, SCLAHE shows superiority in detecting widened PDL abnormalities based on the dentist's visual evaluation (Figure 9). The findings of this research show the CEAs preliminary potential role in highlighting invisible anatomical structures.

References

- [1] K. Thangavel, R. Manavalan, I. L. Aroquiaraj, "Removal of Speckle Noise from Ultrasound Medical Image based on Special Filters: Comparative Study," *ICGST-GVIP Journal*, vol. 9, issue (III), pp. 25–32, 2009
- [2] J. Sijbers, P. Scheunders, N. Bonnet, D.V. Duck, E. Raman, (1996). Quantification and Improvement of the Signal-to-Noise Ratio in a Magnetic Resonance Image Acquisition Procedure, *Magnetic Resonance Imaging* vol. 14, pp. 1157–1163.
- [3] S. A. Ahmad, M. N. Taib, N. E. Khalid, R. Ahmad, H. Taib, "Analysis of Compound Enhancement Algorithms (CEA) based on Adaptive Histogram Equalization (AHE) on Intra-oral Dental Radiographs Images," *International Journal of New Computer Architectures and their Applications (IJNCCA)*, vol. 1, no. 4, pp. 902–916, 2011 (ISSN 2220-9085).
- [4] E. Whaites, "Essentials of Dental Radiographic and Radiology," *Elsevier Science*, 2003.
- [5] Y. Jusman, N. A. M. Isa, R. Kurnia, "A Proposed System for Edge Mammogram Image," *Proceeding of the 9th WSEAS International Conference on Application of Electrical Engineering*, pp. 117–123, 2010.
- [6] S. A. Ahmad, M. N. Taib, N. E. Khalid, R. Ahmad, H. Taib, "The Effect of Sharp Contrast-Limited Adaptive Histogram Equalization (SCLAHE) on Intra-oral Dental Radiograph Images, 2010 IEEE EMBS Conference on Biomedical & Sciences (IECBES 2010).
- [7] B. G. Baksi, E. Alp, E. Sogur, A. Mert, "Perception of anatomical structures in digitally filtered and conventional panoramic radiographs: a clinical evaluation," *Dentomaxillofacial Radiology*, vol. 39, pp. 424–430, 2010.
- [8] M. Mehdizadeh, S. Dolatyar, "Study of Effect of Adaptive Histogram Equalization on Image Quality in Digital Preapical Image in Pre Apex Area," *research Journal of Biological Science*, vol. 4, issue 8, pp. 922–924, 2009.
- [9] W. E. G. W. Alves, E. Ono, J. L. O. Tanaka, E. M. Filho, L. C. Moraes, M. E. L. Moraes, J. C. M. Castilho, "Influence of image filters on the reproducibility of measurements of alveolar bone loss," *Journal of Applied Oral Science*, vol. 4(6), pp. 415–420, 2006.
- [10] T. Sund, A. Moystad, "Sliding window adaptive histogram equalization in intraoral radiographs: effect on image quality," *Dentomaxillofacial Radiology*, vol. 35, pp. 133–138, 2006.
- [11] S. Yalcinkaya, A. Kunze, R. Willian, M. Thoms, J. Becker, "Subjective image quality of digitally filtered radiograph acquired by the Durr Vistascan system compared with conventional radiographs," *Oral Surg Oral Med. Pathol. Oral Radiol. Endod.* vol. 101, pp. 643–651, 2006.
- [12] F. Gijbels, A. M. D. Meyer, C. B. Serhal, C. V. d. Bossche, J. Declerck, M. Persoons, R. Jacob, "The subjective image quality of exact digital and conventional panoramic radiography," *Journal of Clinical Oral Investigation*, vol. 4, pp. 162–167, 2000.
- [13] P. Sprawls, "The Physical Principles of Medical Imaging," Sprawls Educational Foundations, Open Resources for Learning and Teaching, <http://www.sprawls.org/ppmi2/NOISE/>. Accessed on 23rd Oct. 2011.
- [14] T. Ozen, A. Cebeci, C. S. Paksoy, "Interpretation of chemically created periapical lesion using 2 different dental cone-beam computerized tomography units, and intraoral digital sensor, and conventional film," *Oral Surg. Oral Med. Oral Pathol. Oral Radiol. Endod.* vol. 107, no. 3, pp. 426–432, 2009.
- [15] J. A. Regezi, "Periapical Disease: Spectrum and Differentiating Features," *Journal of The California Dental Association*, 1999.
- [16] E. Katsoni, I. A. Tsalafoutas, P. Gritsalis, E. Stefanou, E. Georgiou, E. Yakoumakis, "Exploring the useful expose range limit of three intraoral image receptors for various tube potential, tube current and expose time settings," *Science Research Journal*, vol. 3 no. 5, pp.

- 292–299, 2011. (Open access: <http://www.scirp.org/journal/health/>)
- [17] M. A. Yousuf, Rakib, “An Effective Image Contrast Enhancement Method Using Global Histogram Equalization,” *Journal of Scientific Research*, vol. 3, pp. 43–50, 2011.
- [18] N. Kanwal, A. Girdhar, S. Gupta, “Region Based Adaptive Contrast Enhancement of Medical X-ray Images,” *International Conference on Bioinformatics and Biomedical Engineering*, pp. 1–5, 2011.
- [19] U. Sinha, A. Ton, A. Yaghmai, R. K. Taira, H. Kangarloo, “Image Content Extraction: Application to MR Images of the Brain,” *Radiological Society of North America*, vol. 21, no. 2, pp. 535–547, 2001.
- [20] A. R. Hunsaker, I. B. Oliva, T. Cai, B. T. Dickenson, R. R. Gill, H. Hatabu, F. J. Rybicki, “Contrast Opacification Using a Reduced Volume of Iodinated Contrast Material and Low Peak Kilvoltage in Pulmonary CT Angiography: Objective and Subjective Evaluation,” *American Roentgen Ray Society*, vol. 195, pp. W118–W124, 2010.
- [21] Y. S. Kim, S. E. Jung, B. G. Choi, Y. R. Shin, S. S. Hwang, Y. M. Ku, Y. S. Lim, J. M. Lee, “Image Quality Improvement after Implementation of a CT Accreditation Program,” *Korean Journal of Radiology*, vol. 11, no. 5, pp. 553–559, 2010.
- [22] J. Leipsic, G. Nguyen, J. Brown, D. Sin, J. R. Mayo, “A Prospective Evaluation of Dose Reduction and Image Quality in Chest CT using Adaptive Statistical Iterative Reconstruction,” *American Roentgen Ray Society*, vol. 195, pp. 1095–1099, 2010.
- [23] H. Higashihara, K. Osuga, T. Ueguchi, H. Onishi, H. Tanaka, N. Maeda, K. Tomoda, N. Tomiyama, “Usefulness of contrast-enhanced three-dimensional MR angiography using Arteriovenous Malformations: Initial Experience,” *European Journal of Radiology*, vol. 81, pp. 1134–1139, 2012.
- [24] B. Ardlin, “Transformation-toughened zirconia for dental inlays, crowns and bridges: chemical stability and effect of low-temperature aging on flexural strength and surface structure,” *Dental Material, PubMed*, vol. 18, no. 8, pp. 590–595, 2002.
- [25] L. Ramaglia, L. Sbordone, R. N. Ciaglia, A. Barone, R. Martina, “A clinical comparison of the efficacy and efficiency of two professional prophylaxis procedures in orthodontic patients,” *European Journal of Orthodontics*, vol. 21, pp. 423–428, 1999.
- [26] E. Fung, N. Ewoldsen, H. Germain, D. Marx, C. Miaw, C. Siew, H. Chou, S. Gruinger, D. Meyer, “Pharmacokinetics of bisphenol A released from a dental sealant,” *Journal of American Dental Association*, vol. 131, no. 1, pp. 51–58, 2000.
- [27] J. Pallant, “SPSS Survival Manual, 4th Edition,” Allyn & Unwin, 2011.
- [28] O. E. Langland, R. P. Langlais, J. W. Preece, “Principles of Dental Imaging,” Lippincott Williams & Wilkins, 2002.
- [29] A. Halse, O. Molven, I. Frisstad, “Diagnosing periapical lesions—disagreement and borderline cases,” *International Endodontic Journal*, vol. 35, pp. 703–709, 2002.
- [30] T. Lombardi, M. Bischof, R. Nedir, D. Vergain, C. Galgano, J. Samson, R. Kuffer, “Periapical central giant cell granuloma misdiagnosed as odontogenic cyst,” *International Endodontic Journal*, vol. 39, pp. 510–515, 2006.
- [31] A. Xia, Y. Zhu, X. Wang, “Six cases report of differential diagnosis of periapical disease,” *International Journal of Oral Science*, vol. 3, pp. 153–159, 2011.
- [32] K. Kamburoglu, B. Senel, S. Yuksel, T. Ozen, “A Comparison of the diagnostic accuracy of in vivo and in vitro photostimulable phosphor digital images in the detection of occlusal caries lesion,” *Dentomaxillofacial Radiology*, vol. 30, pp. 17–22, 2010.
- [33] S. E. Stheeman, P. A. Mileman, M. A. Van Hof, P. F. Van Der Stelt, “Diagnostic confidence and accuracy of treatment decisions for radiopaque periapical lesions,” *International Endodontic Journal*, vol. 28, pp. 121–123, 1995. (2007 online).
- [34] S. K. Lanning, P. S. Richards, L. K. McCauley, “Variation in Periodontal Diagnosis and Treatment Planning Among Clinical Instructors,” *Journal of Dental Education*, 2005.
- [35] H. Yoon, Y. Han, H. Hahn, “Image Contrast Enhancement based on Sub-histogram Equalization Techniques without Over-equalization Noise,” *International Journal of Computer Science and Engineering*, vol. 3, no. 2, 2009.
- [36] T. C. Jen, S. Wang, “Histogram Equalization Based on Local Characteristics,” *Proceedings of the 2005 Workshop on Consumer Electronics and Signal Processing (WCESp2005)*, 2005.
- [37] W. Zhiming, T. Jianhua, “A fast implementation of Adaptive Histogram Equalization,” *8th International Conference on Signal Processing (ICSP)*, 2006.
- [38] E. Pisano et al., “Contrast Limits Adaptive Histogram Equalization Image Processing to Improve the Detection of Simulated Spiculations in Dense Mammograms,” *Journal of Digital Imaging*, vol. 11, pp. 193–200, 1998.
- [39] P. Rahmati, G. Hamarneh, D. Nussbaum, A. Adler, “A New Preprocessing Filter for Digital Mammograms,” *Lecture Notes in Computer Science*, vol. 1: 6134, pp. 585–592, 2010.
- [40] P. Jagatheeswari, S. S. Kumar, M. Rajaram, “Contrast Enhancement Based on Histogram Equalization Followed by Median Filter,” *Proceeding of the International Conference on Man-Machine Systems (ICoMMS)*, 2009.
- [41] T. A. Mahmoud, S. Marshall, “Medical Image Enhancement using Threshold Decomposition Driven Adaptive Morphological Filter,” *16th European Signal processing Conference (EUSIPCO)*, 2008.
- [42] R. Kimmel, R. Malladi, N. Sochen, “Images as Embedded Maps and Minimal Surfaces: Movie. Color, Texture and Volumetrics Medical Images,” *International Journal of Computer Vision*, vol. 3992, pp. 111–129, 2000.
- [43] T. Kitasaka, K. Mori, J. Hasegawa, J. Toriwaki, “A Method for Extraction of Bronchus Regions from 3D Chest X-ray CT Images by Analyzing Structural

- Features of the Bronchus,” *FORMA*, vol. 17, no. 4, pp. 321–338, 2002.
- [44] J. C. Junior, A. Kantarci, A. Haffajee, R. P. Teles, R. F. Jr., C. M. Figueredo, “Matrix metalloproteinases and chemokines in the gingival crevicular fluid during orthodontic tooth movement,” *Oxford Journal*, 2011.
- [45] J. E. Botero, A. M. Gonzales, R. A. Mercado, G. Olave, A. Contreras, “Subgingival microbiota in pre-implant mucosa lesions and adjacent teeth in partially edentulous patients,” *Journal of Periodontol*, vol. 76(9), pp. 1490–1495, 2005.
- [46] M. L. M. Zain, I. Elamvazuthi, M. Begam, “Enhancement of Bone Fracture Image Using Filtering Techniques,” *The International Journal of Video and Image Processing and Network Security IJVIPNS*, vol. 9, no. 10, pp. 49–54, 2009.
- [47] N. Kramer, F. G. Garcia, C. Reinelt, A. J. Feilzer, R. Frankenberger, “Nanohybrid vs. fine hybrid composite in extended Class II cavities after six years,” Elsevier, *Dental Material*, vol. 27(5), pp. 455–464, 2011.
- [48] J. Ploeg, E. Giertsen, B. Ludin, C. Morgeli, S. Annelies, S. Zinkernagel, R. Gmur, “Quantitative detection of Porphyromonas gingivalis fim: A genotypes in dental plaque,” Elsevier, pp. 424–430, 2010.
- [49] A. E. Hassanien, J. M. H. Ali, “A Fuzzy-Rule Based Algorithm for Contrast Enhancement of Mammograms Breast Masses,” *4th WSEAS International Conference Information Science, communication and application*, pp. 484–158, 2004.
- [50] M. C. Nicolae, L. A. Moraru, L. Onose, “Comparative Approach for Speckle Reduction in Medical Ultrasound Images,” *Romanian Journal Biophys*, vol. 20, no. 1, pp. 13–21, 2010.
- [51] G. Zentai, “Signal-to-Noise and Contrast Ratio Enhancements by Quasi-Monochromatic Imaging,” *IEEE Transactions on Instrumentation and Measurement*, vol. 60, no. 3, 2011.
- [52] Y. Jusman, N. A. M. Isa, R. Kurnia, “A Proposed System for Edge Mammogram Image,” *Proceeding of the 9th WSEAS International Conference on Application of Electrical Engineering*, pp. 117–123, 2010.
- [53] M. B. Al-Zoubi, A. M. Kamel, M. J. Radhy, “New Spatial Filters for Image Enhancement and Noise Removal,” *Proceeding of the 5th WSEAS International Conference on Applied Computer Science*, pp. 109–113, 2006.
- [54] M. Hazem, N. Mastorakis, “A New Technique for Detecting Dental Disease by using High Speed Neuro-Computers,” *2nd European Computing Conference (ECC ‘08)*, pp. 432–440, 2008.
- [55] R. C. Gonzalez, R. E. Woods, “*Digital Image Processing, Second Edition*,” Prentice Hall, 2001.
- [56] N. M. Noor, N. E. A. Khalid M. H. Ali, A. D. A. Numpang, “Enhancement of Soft Tissue Lateral Neck Radiograph with Fish Bone Impaction Using Adaptive Histogram Equalization (AHE),” *The 2nd International Conference on Computer Research and Development*, 2010.
- [57] J. Poulist, M. Aubin, “*Contrast Limited Adaptive Histogram Equalization (CLAHE)*,” http://radonc.ucsf.edu/research_group/jpouliot/Tutorial/HU/Lesson7.htm, accessed on 4th June 2010.
- [58] R. A. Hummel, “Image Enhancement by Histogram Transformation,” *Computer Graphics and Image Processing*, pp. 184–195, 1977.
- [59] K. Arulmozhi, S. A. Perumal, K. Kannan, S. Bharathi, “Contrast Improvement of Radiographic Images in Spatial Domain by Edge Preserving Filters,” *International Journal of Computer Science and Network Security (IJCSNS)*, vol. 10, no. 2, pp. 233–239, 2010.
- [60] Allen, B. Wilkinson M. *Parallel Programming, Techniques and Applications Using Networked Workstations and Parallel Computers*, Pearson, 2005.
- [61] A. P. Cheim, T. L. Queiroz, W. M. Alencar, R. M. Rezende, E. F. Vencio, “Mesenchymal chondrosarcoma in the mandible: report of a case with cytological findings,” *Journal of Oral Science*, vol. 53, no. 2, pp. 245–247, 2011.
- [62] J. D. Rubenstein, J. G. Li, S. Majumdar, R. M. Henkelman, “Image Resolution and Signal-to-Noise Ratio Requirements for MR Imaging of Degenerative Cartilage,” *American Roentgen Ray Society*, vol. 169, pp. 1089–1096, 1997.